Author's Accepted Manuscript

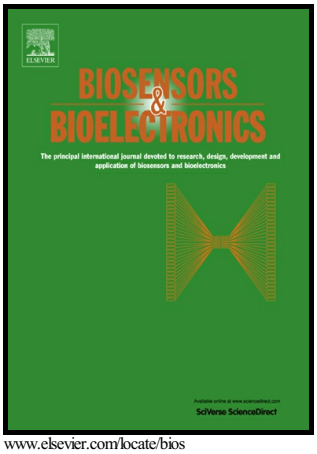

www.elsevier.com/locate/bios

CMOS-compatible biosensor for L-carnitine detection

M.S. Andrianova, E.V. Kuznetsov, V.P. Grudtsov, A.E. Kuznetsov

PII: S0956-5663(18)30547-5
DOI: https://doi.org/10.1016/j.bios.2018.07.044
Reference: BIOS10633

To appear in: *Biosensors and Bioelectronic*

Received date: 7 May 2018
Revised date: 11 July 2018
Accepted date: 22 July 2018

Cite this article as: M.S. Andrianova, E.V. Kuznetsov, V.P. Grudtsov and A.E. Kuznetsov, CMOS-compatible biosensor for L-carnitine detection, *Biosensors and Bioelectronic,* https://doi.org/10.1016/j.bios.2018.07.044

CMOS-compatible biosensor for L-carnitine detection

Andrianova M.S.[a*], *Kuznetsov E.V.*[a], *Grudtsov V.P.*[a], *Kuznetsov A.E.*[a]

[a] Scientific-Manufacturing Complex Technological Centre, 124498, Shokina square, h. 1, bld. 7, Zelenograd, Moscow, Russia

* E-mail: smariika1987@gmail.com

Abstract

A CMOS-compatible ISFET with a Ta_2O_5 sensitive surface was developed. The structure was optimized for achieving high sensitivity using a subthreshold operation mode and by reducing the influence of the capacitances on the value of subthreshold swing. The developed ISFET was used as a basis for a biosensor for L-carnitine detection. To this end, carnitine acetyltransferase was immobilized on the ISFET sensitive surface. The immobilized enzyme was active (0.082 U/g $_{\text{model plate}}$). The complete microsystem, consisting of a packaged chip, an immobilized enzyme and a microfluidic channel, detected L-carnitine at a range of 0.2-100 μM with a LOD of 0.2 μM. The biosensor response was linear in the range of 0.2-50 μM of L-carnitine with sensitivity 18.0±1.7 mV/μM. An experiment with artificial urine containing 1.3 μM L-carnitine showed that the proposed biosensor could be used on a real sample. Therefore, a new sensor specially optimized for biosensing CMOS-compatible ISFET structures and direct determination of L-carnitine with immobilized carnitine acetyltransferase was developed.

Keywords: biosensor, ion-sensitive field-effect transistor (ISFET), carnitine acetyltransferase, L-carnitine, Ta_2O_5

1. Introduction

L-carnitine plays an important role in the transport of fatty acids across the inner mitochondria membrane for subsequent β-oxidation (Bremer, 1983; Rebouche and Paulson, 1986). L-carnitine also modulates the intramitochondrial balance between coenzyme A (CoA) and acetyl-coenzyme A (acetyl-CoA), buffering excess acetyl-CoA in skeletal muscle during exercise (Ramsay et al., 2001). Another additional role of L-carnitine is removing the toxic effects of poorly metabolized acyl groups by excreting these substances as carnitine esters (Vaz and Wanders, 2002) and participating in peroxisomal β-oxidation (Jakobs and Wanders, 1995). Inborn errors of L-carnitine metabolism comprise a group of genetic diseases linked to the dysfunctionality of L-carnitine transporters and transferases (Sharma and Black, 2009) that lead to cardiomyopathy and hypoglycaemia and have been associated with the high morbidity and mortality of newborns (Cox, 2007; Schimmenti et al., 2007). In addition to genetic diseases, L-carnitine deficiency is commonly observed in chronic haemodialysis patients (Sakurabayashi et

al., 2008) and has been associated with methylmalonic (HOrster and Hoffmann, 2004), hypoketotic hypoglycaemic encephalopathy (Breningstall, 1990), chronic fatigue syndrome (Plioplys and Plioplys, 1995) and isovaleric acidaemia (Chalmers et al., 1984). L-carnitine deficiency may be caused by chronic conditions, such as diabetes mellitus, heart failure, Alzheimer disease (Evangeliou and Vlassopoulos, 2003), or even drug administration (Murphy et al., 1985). Thus, L-carnitine has become a "conditionally essential nutrient" or "conditional vitamin" in medical treatment (Arduini et al., 2008). Therefore, L-carnitine measurement for screening disorders in fatty acid oxidation or for precise control in patients with L-carnitine supplementation is critically important in modern medical applications (El-Hattab et al., 2010; Ramsay et al., 2001; Zammit et al., 2009).

Currently, different methods of D/L-carnitine determination have been developed, including UV/VIS spectrophotometry, fluorometry, radioassays, electrochemical sensors, chromatography and mass-spectrometry techniques (Da□browska and Starek, 2014). The comprehensive review of chromatographic and mass-spectrometry methods for carnitine detection is presented by (Mansour et al., 2013) and (Da□browska and Starek, 2014). Spectrophotometric methods are typically based on monitoring NADH during the enzymatic reaction of L-carnitine dehydrogenase (Matsumoto et al., 1990; Obón et al., 1999; Takahashi et al., 1994), and an alternative method is based on colorimetric visualization of CoA by the addition of 5,5'-dithiobis-2-nitrobenzoate during carnitine transferase reactions (Prieto et al., 2006; Wan and Hubbard, 1998). Spectrophotometric methods for the determination of L-carnitine have significant limitations, especially when working with actual samples (blood, urine), which have high background absorption and may contain interfering substances. Another method is based on the radioassay of labelled C^{14}-acetylcarnitine generated during carnitine acetyltransferase reaction (Cederblad and Lindstedt, 1972). However, this method requires radiolabelled reagents, specially trained personal and licenses to handle radioactive material. Electrochemical methods for L-carnitine determination use carnitine dehydrogenase and are coupled with another enzymatic reaction: diaphorase (Comtat et al., 1988) and salicylate hydroxylase (Chen et al., 2008). In these methods, NADH was generated by dehydrogenase and then was oxidized in a second reaction that can be detected by electrodes. Rat'ko A. A. et al. developed vancomycin and teicoplanin-based selective membranes for potentiometric electrodes for the selective detection of L-carnitine (Stefan-Van Staden et al., 2009). Selective membranes for the potentiometric detection of L-carnitine via a molecular-imprinted technique have been reported by Moret J. et al. (Moret et al., 2014). However, most electrochemical methods of carnitine detection are not direct, particularly with the use of enzymes; these methods could generate false-positive signals because of the oxidation/reduction of concomitant organic

compounds. Thus, it is a serious challenge to use these detection techniques for the analysis of complex mixtures with unknown compositions.

Complementary metal oxide semiconductor (CMOS)-integrated circuit technology is an attractive and inexpensive platform for the implementation of electrochemical microsensors (Chandra, 2016; Lei et al., 2016; Mahato et al., 2018; Tran et al., 2018). Compared to traditional electrochemical methods, CMOS biosensors provide lower costs, lower power consumption and smaller sizes. Ion-sensitive field-effect transistor (ISFET) can be described as a conventional metal-oxide-semiconductor-FET (MOSFET) device, where the metallic gate is replaced by an ionic conductive electrolyte (Kokot and Ossowski, 2009). ISFETs are fabricated in a standard CMOS process without additional post-processing steps, which reduces production costs and enables miniaturization for a more compacted form. ISFETs are ideal platforms for DNA sequencing (Rothberg et al., 2011) for the detection of neuronal activities (Grattarola and Martinoia, 1993), cellular population monitoring (Martinoia et al., 2001) and environmental studies (Jimenez-Jorquera et al., 2010).

The carnitine acetyltransferase (CAT, EC 2.3.1.7) is an enzyme responsible for the selective catalysis of acetyl transfer between coenzyme A and L-carnitine (Colucci and Gandour, 1988; Ramsay and Naismith, 2003). The pigeon-breast muscle CAT is well studied and commercially available. The maximum activity of this CAT is towards the transfer of acetyl groups compared to other acyl groups. Therefore, the pigeon-breast muscle CAT was selected as sensitive part of a constructed biosensor.

Combination of ISFET and CAT allows to obtain a new sensor for measurement of L-carnitine. CAT provides high specificity towards L-carnitine and ISFET enables to detect the reaction directly without additional reagents. The proposed approach supports the concept of point-of-care diagnostics (PoCD), where the whole sensor may be designed as a portable device with simple semi-automated measurements; it requires small sample volumes with minimum probe preparation, that overall impact the price of analysis.

Here, we report a new sensor based on specially optimized for biosensing CMOS-compatible ISFET structures and immobilized carnitine acetyltransferase for the direct determination of L-carnitine (Fig. 1). We provided the first evidence that ISFET can be used for the detection of carnitine acetyltransferase reactions and the determination of L-carnitine.

Fig. 1

Fig. 1. Final ISFET structure and enzymatic reaction.

2. Materials and methods

2.1. Materials

Carnitine acetyltransferase (CAT, EC 2.3.1.7) from pigeon breast muscle was obtained from Sigma Aldrich CAS Number 9029-90-7 (USA). The measured activity of CAT (AcCoA and L-carnitine) was 10 U/ml. Phosphoric acid solution, petroleum jelly, (3-aminopropyl) triethoxysilane (APTES), mineral oil, L-carnitine hydrochloride, O-acetyl-L-carnitine hydrochloride, acetyl coenzyme A lithium salt, coenzyme A sodium salt hydrate were purchased from Sigma Aldrich (USA). Glutaric dialdehyde was purchased from Merck (USA). Epoxy resin HT2 and its hardener were obtained from PoxySystems (Germany). Methanol and hexane were purchased from Khimmed (Russia). Microcrystalline wax SP-19 was obtained from Strahl and Pitsch (USA). All external components (hoses and connectors) of the microfluidic system were obtained from microfluidic ChipShop (Germany).

2.2. ISFET fabrication and package

Fabrication of n-type ISFET was integrated into standard 1.2-μm CMOS (p-type Si wafers, 12–22 Ohm·cm resistivity) technology in SMC "Technological Centre", Russia. ISFET structures were formed after CMOS transistor formation and before the standard metallization step. To this end, 50 nm of tantalum (Ta) was deposited by PVD onto 10 nm SiO_2 gate dielectric obtained using wet oxidation in oxygen at 850°C for 10 min. Tantalum deposition is done after MOSFET fabrication, as Ta does not withstand high-temperature operations (such as oxidation and annealing at 850°C). After the completion of metallization and passivation steps, the tantalum gate area was opened by wet etching. The tantalum film was oxidized to Ta_2O_5 in deionized H_2O at 50°C for 10 min. An external reference electrode of Ag/AgCl (in the open system) or gold wire (in the microfluidic system) was used as a gate contact. All measurements were performed on transistors with a channel size of 100 × 6 μm.

The package of the fabricated ISFET included a number of operations: cutting of wafer into separate chips; attaching of chips to the package base with K-400 glue; aluminium wire (diameter of 27 μm) bonding; integration of reference electrode (bonding of Au wire with the diameter of 30 μm) and chipping of the packaging lead-frame (Gubanova et al., 2017).

Two structures formed on the surface of the ISFET were used during the study: structures made of epoxy in form of a “well” on the non-packaged ISFET and a microfluidic system (MFS) on the packaged ISFET resin using direct ink writing approach. The procedure of structures formation is described in details in (Gubanova et al., 2017).

2.3. Carnitine acetyltransferase activity assay

CAT activity was measured spectrophotometrically. Buffer solution (100 mM Na_2HPO_4/NaH_2PO_4, pH 7.8), substrate solution (0.18 mM acetyl coenzyme A/coenzyme A and

5.4 mM L-carnitine/ O-acetyl-L-carnitine), and enzyme solution (0.6 U/ml in reaction mixture) were placed into wells of a microtitre plate (total volume of 150 μL), and the absorbance at 233 nm was measured using a Tecan Infinite M200 microplate reader (Austria). The initial reaction rate and enzyme activity were detected based on increase or decrease of acetyl coenzyme A (ε = 4.5 $mM^{-1}см^{-1}$) with a 4.3-mm optical path length. One unit will convert 1.0 μmol of O-acetyl-L-carnitine and CoA to L-carnitine and acetyl-CoA or L-carnitine and acetyl-CoA to O-acetyl-L-carnitine and CoA per minute at pH 7.8 at 25°C.

The activity of CAT immobilized on the surface of the model plates ($Ta+Ta_2O_5$, 4 × 4 mm, 16–19 mg) was measured using similar conditions. Plates were incubated in wells of the microtitre plate with 150 μL of reaction mixture, and then the samples were extracted by tweezers, and the decrease or increase in O-acetyl-L-carnitine concentration was spectrophotometrically measured. Subsequently, the plates were returned to the wells and the enzymatic reaction was continued. The total measurement time was ~100 min. The activity of immobilized CAT was calculated according to the weight of the plates (U/mg).

2.4. Immobilization of the enzyme on the surface of plates

The model wafer, which had an ultrathin Ta_2O_5 surface identical to the ISFET sensitive surface, was used as a model substrate for immobilization. Immobilization of the enzyme was conducted in three stages: the plates were incubated with 3% APTES methanol solution for 1 h at 22°C, immersed in solution of 5% glutaric dialdehyde in water for 4 h at 22°C, and then incubated in an enzyme solution (0.025 mg/ml) for 17 h at 1°C. The plates were thoroughly rinsed between the stages.

The ISFET-sensitive surface in the MFS chamber was modified using a similar procedure, and the necessary reagents were delivered with syringes.

The storage stability of the immobilized CAT was also investigated. Plates with immobilized enzyme were stored in 0.1 M Na_2HPO_4/NaH_2PO_4 (pH 7.0) at 1°C. And every 2-3 days the activity of the plates with immobilized enzyme was measured according section 2.5.

The AFM study was performed on a Bruker Dimension ICON probe-scanning microscope (USA). Probes of the DNP-S series (Bruker, USA) in tapping mode were used to obtain the 500×500 nm (256 dots per line) images. Built-in functions of the Nanoscope Analysis software were used for image processing.

2.5. Biosensor measurement: operating mode and output response

I-V curves (dependence of drain current I_{ds} on the reference electrode voltage V_g) of the ISFET were recorded using an Agilent B1500A semiconductor device parameter analyser (USA)

and Cascade PM5 probe station (USA) with Agilent VEE Pro. The threshold voltage V_t and subthreshold swing S were extracted and used to set the ISFET in subthreshold mode. Time-dependent changes in the current I_d (V_g=const, V_{ds} = 0.1 V) were recorded and surface potential change $\Delta\varphi_i \approx \frac{S}{S_0}\varphi_t \frac{I_{i+1}-I_i}{I_i}$ was used as a signal independent of transistor parameters (Andrianova et al., 2016).

Reagent delivery to the sensitive surface of the biosensor was performed by two 2.5-ml syringes (neMESYS Syringe Pump station, Germany) that enabled continuous flow of the solution with the possibility of switching the flow between pumps. The first pump was filled with buffer solution (20 mM Na_2HPO_4/NaH_2PO_4 (pH 7.9)), and the second pump was filled with a solution of AcCoA (final concentration 80 μM) and carnitine (concentration range from 10^{-7} to 10^{-4} M) in the same buffer or diluted artificial urine (artificial urine: 200 mM urea, 54 mM NaCl, 5 mM citric acid, 15 mM NH_4Cl, 3 mM $CaCl_2$, 2 mM $MgSO_4$, 2 mM $NaHCO_3$, 3.6 mM NaH_2PO_4, and 0.4 mM Na_2HPO_4, pH was adjusted by 0.5 M NaOH to 6.2). The flow rate was 0.5 μl/s.

To study the ISFET response, the corresponding buffer solution was pumped through the finished system within ~300 s to regulate the source-drain of the transistor in time. Then, the flow was switched to the other pump filled in with a solution containing L-carnitine and pumped for 300 s. Subsequently, the flow was stopped and the system was static. During these manipulations, the change in I_d was recorded.

For data processing, surface potential calculations ($I_d \rightarrow \Delta\varphi$) were performed. The signal from the sample was calculated as an absolute value of the difference between baseline and sample addition.

3. Results and Discussion

3.1. ISFET design and characterization

The main goal in designing of ISFET structure was achieving the high sensitivity to changes in surface potential. To this end, ISFET was designed for operation in subthreshold mode, where higher sensitivity to changes in surface potential can be achieved compared to operation in strong inversion (Kaisti, 2017). This finding implies minimizing the value of subthreshold swing (*S*).

Using the expression for MOSFET subthreshold swing ("MOSFETs," 2006) and the analysis of the small-signal equivalent scheme (Fig. 2), an expression for floating gate ISFET subthreshold swing is derived:

$$S = S_0(1+\frac{C_{par}}{C_e}+\frac{C_{fet}}{C_e})(1+\frac{C_b}{C_{Ta_2O_5}+C_{SiO_2}}+\frac{C_i}{C_{Ta_2O_5}+C_{SiO_2}}+\frac{C_{ss}}{C_{Ta_2O_5}+C_{SiO_2}}), \quad (1)$$

where S_0 - ideal subthreshold swing (equal to 60 mV/dec at 300 K), C_b - depletion capacitance, C_i - inversion capacitance, $C_{Ta_2O_5}$ - Ta_2O_5 gate oxide capacitance, C_{SiO_2} - SiO_2 gate oxide capacitance, C_{ss} - interface states capacitance, C_e - electrolyte capacitance, C_{par} - parasitic capacitance, C_{fet} - equivalent capacitance including C_{ox}, C_b, C_i and C_{ss}.

This expression implies a need for the reduction of capacitances C_{par}, C_{fet}, C_b, C_i and C_{ss} to obtain a minimum value of subthreshold swing. Accordingly, the ISFET structure optimization was generated.

In the developed structure, the drain and source are self-aligned with electrolyte gate, which reduces the area of parasitic adsorption and parasitic capacitance C_{par}. This minimizes the effect of gate-drain C_{gd} and gate-source C_{gs} capacitances, which arise from the overlap of gate and drain/source regions. The contact to transistor channel is achieved through n-type inversion regions, which are formed beneath isolating oxide layer by the presence of a fixed charge (the effective fixed charge density of isolating oxide is approximately 10^{12} cm^{-2}). The presence of inversion regions does not degrade current-voltage characteristics of the ISFET as the channel serial resistance in subthreshold mode is substantially larger. Current-voltage characteristics of these structures, through ohmic contact to the gate, were compared to similar transistors with an overlap of gate and drain/source regions, and the average difference in subthreshold swing value was no more than 2 mV/dec.

The bulk carrier concentration in the substrate was maintained as low as possible to minimize subthreshold swing. Lowering the bulk carrier concentration reduces C_b (Schneider and Galup-Montoro, 2010), and, consequently, brings *S* closer to minimum value. Thus, the transistor channel area was not doped and the bulk carrier concentration was 10^{15} cm^{-2}.

Ta_2O_5 was selected as a sensing surface material. ISFETs with Ta_2O_5 gate oxides showed high pH sensitivities, low response times and long-term chemical stability in water solutions (Akiyama et al., 1982; Matsuo and Esashi, 1981; Poghossian, 1992; Van Hal et al., 1996). The thickness of the resulting oxide was estimated by C-V measurements of the electrolyte-tantalum oxide-Ta structure with 0.1 M citrate-phosphate buffer as the electrolyte, thus minimizing the effect of serial electrolyte capacitance. Assuming that the main fraction in the native oxide is Ta_2O_5 with dielectric permittivity in the range of 20-30 (Kerrec et al., 1995), an average oxide thickness of 3-4 nm was found. Thus, the resulting structure was ISFET with a floating Ta gate.

Leakage current through the Ta oxide was negligible in the reference electrode voltage range ±2 V, which is sufficient for ISFET operation mode.

The electrical characterization of the fabricated ISFET started with the measurement of gate leakage I_g, drain current I_d and source current I_s in the buffer in working range [-0.5; +1.5 V]. The reference electrode current was lower than 5 nA at V_g 1.5 V. I_d and I_s were not affected by the leakage current and were symmetrical about the V_g axis. This result indicated that the transistor had the field-effect-transistor properties and could be used for further investigation. I_d-V_g curves of the fabricated ISFET were reproducible and no significant hysteresis (≤ 2 mV) was observed. Compared to similar structures with ohmic contact to the Ta gate, the existence of floating gate in the developed ISFET had no negative effect on the subthreshold swing, and the average value was 82 mV/dec (Fig. 2).

Fig.2a, b

Fig. 2. a - ISFET small-signal equivalent scheme: showing all components and replacing C_{ox}, C_b and C_{ss} by an equivalent capacitance C_{fet}. b - I_d-V_g curve of the fabricated ISFET: gate leakage I_g, drain current I_d and source current I_s in 0.1 M citrate-phosphate buffer, pH 7.08.

Additionally, the ISFET was characterized by measuring pH sensitivity in different buffer solutions: 0.1 M citrate-phosphate buffers and 0.1 M MES/NaOH. For this purpose, the I_d-V_g curve was obtained for each buffer solution, and the dependence of the threshold voltage V_t ($I_d \approx$ 100 nA) on the pH values was determined (Fig. 3a, b). The sensitivity of the fabricated ISFET was ~52 mV/pH, which is close to the theoretical maximum (Matsuo and Esashi, 1981). The values of threshold voltages V_t for different used buffers observed a small voltage drift. The voltage drift was 5 mV, and based on the sensitivity of 52 mV/pH, the drift corresponded to the measurement accuracy of 0.1 pH.

To measure the hysteresis of V_t on pH I-V, curves were recorded in MES/NaOH buffer in the direction of pH 3.40-5.68-6.02-6.39-6.39-6.02-5.68-3.40-3.40-5.68-6.02-6.39 (Fig. 3c). The fabricated ISFET showed a pH drift less than 0.1. Measurements were obtained with the continuous substitution of buffers; the interval between the start and end pH was approximately 1 h.

Fig. 3a, b, c

Fig. 3. a - Typical cyclic I-V curves for the fabricated ISFET with different buffer solutions. b - The dependence of the threshold voltage V_t ($I_d \approx$ 100 nA) on the pH values of different buffer solutions. c - The dependence of V_t on pH recorded in MES/NaOH buffer in the direction of pH 3.40-5.68-6.02-6.39-6.39-6.02-5.68-3.40-3.40-5.68-6.02-6.39.

3.2. Biosensor studies

3.2.1. Enzyme immobilization

The next step of the biosensor fabrication was CAT immobilization on the sensing surface of the ISFET (the tantalum oxide surface) to increase the sensitivity of ISFET to the enzymatic reaction (Komarova et al., 2015). For this purpose, covalent immobilization with the use of glutaric dialdehyde for the formation of Schiff bases with the lysine amino groups of enzymes was used as an immobilization procedure. The immobilization protocol was tested on model plates whose surface was identical to the ISFET sensing surface. Thus, the tantalum oxide surface of the plate was modified in three stages: first, silanization with 3-aminopropyltriethoxysilane (APTES) from methanol; next, spacer bonding with glutaric dialdehyde in water; and then, incubation with the enzyme solution in phosphate buffer (0.1 M Na_2HPO_4/NaH_2PO_4, pH 7.0).

To confirm CAT immobilization, atomic force microscopy (AFM) was performed on the Ta_2O_5 sensitive surface before and after the procedure (Fig. 4). This study revealed that original roughness had changed from the smooth surface with Ra = 0.112 nm to Ra =0.476 nm with the formation of associates, which are typical for enzymatic film formation on the surface.

Fig. 4

Fig. 4. The AFM image of the surface of Ta_2O_5 before and after immobilization of the enzyme.

Activity assays of the model plates showed that immobilized CAT was catalytically active and the activity of the plates was 0.082 U/g (CoA and acetyl-l-carnitine were used as substrates). Analysis of the storage stability (0.1 M Na_2HPO_4/NaH_2PO_4, pH 7.0, T = 1°C) revealed that the plates remained active for 10 days while maintaining 15% of initial activity. To increase the stability of the immobilized CAT, the source of the enzyme can be changed or protein engineering can be used to modify enzyme properties. In addition, various immobilization approaches can be employed to determine the technique most suitable for the immobilization of this enzyme with long-term preserving of maximum activity.

Further immobilization procedure with glutaric dialdehyde was used for modification of the ISFET sensitive surface.

3.2.2. Biosensor investigation

For the convenient use of the biosensor and further integration into signal processing systems, a microfluidic system (MFS) was formed on the chip surface using a sacrificial layer technique (Lewis, 2006). The MFS also eliminated the problem of evaporation of reagents and

liquid spills on the contacts under voltage. The immobilization of the CAT on the sensitive surface of ISFET was performed through the MFS using hoses and syringes for reagent delivery.

The biosensor was tested towards enzymatic reaction in the range of 0.1–100 μM of L-carnitine, while the concentration of CoA was constant and equalled 80 μM (Fig. 5a). The increase in surface potential was observed when all the components were present in the gate solution, verifying that this response was due to the enzymatic reaction. The used CAT catalyses a reversible transfer reaction of acetyl group between CoA and L-carnitine. The enzymatic reaction is an acid-base catalytic reaction with a random order of substrate binding. During reaction the stabilization of oxyanion in catalytic centre occurred (Colucci and Gandour, 1988; Hsiao et al., 2004; Ramsay and Naismith, 2003). This charged anion, as well as local pH-change during catalysis, may be detected by ISFET when the enzyme was immobilized on the sensitive surface (Fig. 1). The specificity of the fabricated sensor is determined mostly by the substrate specificity of the enzyme, which was studied earlier (Colucci and Gandour, 1988). It is known that CATs are highly specific enzymes for carnitine.

As a response of the biosensor to different concentrations of L-carnitine, the value of the surface potential ($\Delta\varphi_S$) at 600 s for each concentration was taken. The dependence of these values on the concentration of L-carnitine is presented on the graph (Fig. 5b). Thus, the LOD of L-carnitine was 0.2 μM and the biosensor response (surface potential change, $\Delta\varphi_S$) was linear in the range of 0.2-50 μM of L-carnitine in semi-logarithmic coordinates with sensitivity 18.0±1.7 mV/μM (Fig. 5b). The biosensor described showed good operation stability: 15 ml of the solution passed through the inner chamber of MFS (0.5 μl/s), which is approximately 2 μl in volume, with continuous measurement of different L-carnitine concentrations. The sensor retained 75% of initial activity. Thus, the sensor could maintain its excellent performance for detection of L-carnitine.

Determination of L-carnitine in artificial urine showed that the fabricated biosensor performed very well. A sample of artificial urine containing initially 20 μM of L-carnitine was diluted 15-fold with a working measurement buffer to minimize the matrix effect and provide conditions for the functioning of the enzyme. Thus, the solution entering the sensor contained 1.3 μM of L-carnitine. As shown in Fig. 5, the point lies in the required range on the calibration curve.

Fig. 5a, b

Fig. 5. a - Real-time signal of the enzyme-modified ISFET (in $\Delta\varphi$) after L-carnitine addition at different concentrations, 80 μM of AcCoA. Data are normalized. b - Semi-logarithmic dependence of the ISFET response $\Delta\varphi_s$ (at 600 s) to the addition of L-carnitine: ■ – calibration

curve for different L-carnitine concentrations, ● – L-carnitine (1.3 μM) in artificial urea. Error bars were calculated taking into account three different measurements of each point on the separate biosensors.

Typically, urine collections are analysed for nonesterified and total L-carnitine (Rebouche, 2004). The amount of carnitine is correlated with creatinine (μmol/$g_{creatinine}$) (Chalmers et al., 1984; Rebouche, 2004). Normal values of free L-carnitine – 7-128 μmol/$g_{creatinine}$, acyl-L-carnitines – 24-127 μmol/$g_{creatinine}$, and acyl/free ratio – 0.7-3.4 (Chalmers et al., 1984). Higher normal values were shown in the article (Schmidt-Sommerfeld et al., 1989): free L-carnitine – 90-369 μmol/$g_{creatinine}$ and total L-carnitine – 210-535 μmol/$g_{creatinine}$. Considering the level of creatinine in 24-h urine samples from men (955-2936 mg) and women (601-1689 mg) (https://www.mayomedicallaboratories.com/test-catalog/Clinical+and+Interpretive/8513) and the mean volume in 1.5 L of urine (Paterson, 1967), the concentration of free L-carnitine in urine is in the range ~ 2.7-722 μM, while total L-carnitine is in the range ~ 14.7-1047 μM. Thus, subject to the dilution of urine with the working buffer, the proposed biosensor operates in the required range.

Compared with other methods for carnitine detection presented in Table 1, the obtained biosensor showed equal or better performance. The LODs of carnitine are mostly in the range of micromolar units (Desiderio et al., 2008; Pormsila et al., 2010; Prieto et al., 2006; Takahashi et al., 1994), and the described biosensor showed a better detection limit. Additionally, the present approach had greater potential for miniaturization and creation of sensors for individual use because it did not require expensive and complex devices (such as a mass spectrometer). Furthermore, the fabricated biosensor provided a fast response (600 s), even at low L-carnitine concentrations, in contrast to mass spectrometric methods, which require considerable time for signal accumulation.

Table 1. Analytical methods for carnitine detection presented in the literature

Method	LOD, μM	Range, μM	Analysis time, min	Reaction volume, μL	Ref.
Solid phase extraction with tandem mass spectrometer	0.07	-	19	10, 40	(Hirche et al., 2009)
A capillary electrophoresis with tandem mass spectrometry	2	20–160	22	1120	(Desiderio et al.,

					2008)
A capillary electrophoresis with electrochemical detection	2.6	5–500	4	200	(Pormsila et al., 2010)
Enzymatic assay with carnitine dehydrogenase with spectrophotometric detection (λ = 450 nm)	5	5-250	9	50	(Takahashi et al., 1994)
Enzymatic assay with carnitine acetyltransferase with spectrophotometric detection (λ = 412 nm)	1.7	1.7-310	10	1000	(Prieto et al., 2006)
Potentiometric membrane electrodes based on teicoplanin modified with acetonitrile	7.64	10-10000	0.5–1	100000	(Stefan-Van Staden et al., 2009)
Amperometric detection with carnitine dehydrogenase	-	100-10000	2	3	(Comtat et al., 1988)
Radio-enzymatic assay with carnitine acetyltransferase	0.11	up to 15	85	900-1450	(Seline and Johein, 2007)
Potentiometric selective membranes with molecularly-imprinted polymer for carnitine	77-90	down to 4	3	20-5000	(Moret et al., 2014)
ISFET with immobilized carnitine acetyltransferase	0.2	0.2-100	5-10	2 (inner chamber)	This work

Thus, the biosensor based on n-channel ISFET and CAT for detection of L-carnitine was fabricated. The biosensor had good operating characteristics and enabled the determination of L-carnitine in artificial urine. The main limitation of the biosensor is low enzyme-carnitine acetyltransferase stability. This limitation may be overcome by protein engineering, using another enzyme source, or optimization of the immobilization technique. Also, it is still a difficult task to fabricate ISFET with sensitive surface that allows to detect low signal on baseline drift over time.

4. Conclusions

A biosensor based on enzyme-modified ISFET for the detection of L-carnitine was developed for the first time. The use of a newly fabricated CMOS-compatible ISFET with a Ta_2O_5-sensitive surface was fabricated for high sensitivity measurements using a subthreshold operation mode and by reducing the influence of the capacitances on the value of subthreshold swing. The pH-sensitivity of the fabricated ISFET (~52 mV/pH) is close to theoretical one. The biosensor, consisting of immobilized carnitine acetyltransferase on the sensitive ISFET surface and microfluidic system on the top of the chip, showed fast analytic response and can be easily integrated into portable devices for rapid assay. The LOD of L-carnitine for this biosensor was 0.2 μM, response was linear in the range of 0.2-50 μM of L-carnitine with sensitivity of 18.0±1.7 mV/μM. The described biosensor enabled the determination of L-carnitine in artificial urine, which makes this sensor suitable for measuring real samples.

Acknowledgement

This work was supported by the Russian Science Foundation (project #17-79-20383).

References

Akiyama, T., Ujihira, Y., Okabe, Y., Sugano, T., Niki, E., 1982. Ion-sensitive field-effect transistors with inorganic gate oxide for pH sensing. IEEE Trans. Electron Devices 29, 1936–1941.

Andrianova, M., Gubanova, O., Komarova, N. , Kuznetsov, E., Kuznetsov, A., 2016. Development of a biosensor based on phosphotriesterase and n-channel ISFET for detection of pesticides. Electroanalysis 28, 1311–1321.

Arduini, A., Bonomini, M., Savica, V., Amato, A., Zammit, V., 2008. Carnitine in metabolic disease: potential for pharmacological intervention. Pharmacol. Ther. 120(2), 149-156.

Bremer, J., 1983. Carnitine--metabolism and functions. Physiol. Rev. 63, 1420–1480.

Breningstall, G., 1990. Carnitine deficiency syndromes. Pediatr. Neurol. 6(2), 75-81.

Cederblad, G., Lindstedt, S., 1972. A method for the determination of carnitine in the picomole range. Clin. Chim. Acta 37, 235–243.

Chalmers, R., Roe, C., Stacey, T., Hoppel, C., 1984. Urinary excretion of l-carnitine and acylcarnitines by patients with disorders of organic acid metabolism: Evidence for secondary insufficiency of l-carnitine. Pediatr. Res. 18, 1325–1328.

Chandra, P., 2016. Nanobiosensors for personalized and onsite biomedical diagnosis. IET Digital Library. 638.

Chen, Z., Warsinke, A., Gajovic, N., Große, S., Hu, J., Kleber, H.-P., Frieder W., 2008. A D-carnitine dehydrogenase electrode for the assessment of enantiomeric purity of L-carnitine preparations. Anal. Lett. 33, 1079–1089.

Colucci, W., Gandour, R., 1988. Carnitine acetyltransferase: a review of its biology, enzymology, and bioorganic chemistry. Bioorg. Chem. 16(3), 307-334.

Comtat, M., Galy, M., Goulas, P., Souppe, J., 1988. Amperometric bienzyme electrode for l-carnitine. Anal. Chim. Acta 208, 295–300.

Cox, G., 2007. Diagnostic approaches to pediatric cardiomyopathy of metabolic genetic etiologies and their relation to therapy. Prog. Pediatr. Cardiol. 24(1), 15-25.

Dabrowska, M., Starek, M., 2014. Analytical approaches to determination of carnitine in biological materials, foods and dietary supplements. Food Chem. 142, 220-232.

Desiderio, C., De Rossi, A., Inzitari, R., Mancinelli, A., Rossetti, D.V., Castagnola, M., Messana, I., 2008. Optimization of a rapid capillary electrophoresis ESI-IT tandem mass spectrometry method for the analysis of short-chain carnitines in human plasma. Anal. Bioanal. Chem. 390, 1637–1644.

El-Hattab, A., Li, F., Shen, J., Powell, B., Bawle, E., Adams, D., Wahl, E., Kobori, J., Graham, B., Scaglia, F., Wong, L., 2010. Maternal systemic primary carnitine deficiency uncovered by newborn screening: clinical, biochemical, and molecular aspects. Genet. Med. 12, 19–24.

Evangeliou, A., Vlassopoulos, D., 2003. Carnitine metabolism and deficit - when supplementation is necessary? Curr. Pharm. Biotechnol. 4, 211–219.

Grattarola, M., Martinoia, S., 1993. Modeling the Neuron-Microtransducer Junction: From Extracellular to Patch Recording. IEEE Trans. Biomed. Eng. 40, 35–41.

Gubanova, O., Andrianova, M., Saveliev, M., Komarova, N., Kuznetsov, E., Kuznetsov, A., 2017. Fabrication and package of ISFET biosensor for micro volume analysis with the use of direct ink writing approach. Mater. Sci. Semicond. Process. 60, 71–78.

Hirche, F., Fischer, M., Keller, J., Eder, K., 2009. Determination of carnitine, its short chain acyl esters and metabolic precursors trimethyllysine and γ-butyrobetaine by quasi-solid phase extraction and MS/MS detection. J. Chromatogr. B Anal. Technol. Biomed. Life Sci. 877, 2158–2162.

Horster, F., Hoffmann, G., 2004. Pathophysiology, diagnosis, and treatment of methylmalonic aciduria - recent advances and new challenges. Pediatr. Nephrol. 19(10), 1071-1074.

Hsiao, Y., Jogl, G., Tong, L., 2004. Structural and biochemical studies of the substrate selectivity of carnitine acetyltransferase. J. Biol. Chem. 279, 31584–31589.

https://www.mayomedicallaboratories.com/test-catalog/Clinical+and+Interpretive/8513

Jakobs, B., Wanders, R., 1995. Fatty acid β-oxidation in peroxisomes and mitochondria: The first, unequivocal evidence for the involvement of carnitine in shuttling propionyl-CoA from peroxisomes to mitochondria. Biochem. Biophys. Res. Commun. 213, 1035–1041.

Jimenez-Jorquera, C., Orozco, J., Baldi, A., 2010. ISFET based microsensors for environmental monitoring. Sensors. 10(1), 61-83.

Kaisti, M., 2017. Detection principles of biological and chemical FET sensors. Biosens. Bioelectron. 98, 437-448.

Kerrec, O., Devilliers, D., Groult, H., Chemla, M., 1995. Dielectric properties of anodic oxide films on tantalum. Electrochim. Acta 40, 719–724.

Kokot, M., Ossowski, T., 2009. Excitation-independent constant conductance isfet driver. Metrol. Meas. Syst. 16, 631–639.

Komarova, N., Andrianova, M., Gubanova, O., Kuznetsov, E., Kuznetsov, A., 2015. Development of a novel enzymatic biosensor based on an ion-selective field effect transistor for the detection of explosives. Sensors Actuators, B Chem. 221, 1017–1026.

Lei, K.-M., Mak, P.-I., Law, M.-K., Martins, R.P., 2016. CMOS biosensors for in vitro diagnosis – transducing mechanisms and applications. Lab Chip 16, 3664–3681.

Lewis, J., 2006. Direct ink writing of 3D functional materials. Adv. Funct. Mater. 16, 2193–2204.

Mahato, K., Kumar, A., Maurya, P., Chandra, P., 2018. Shifting paradigm of cancer diagnoses in clinically relevant samples based on miniaturized electrochemical nanobiosensors and microfluidic devices. Biosens. Bioelectron. 100, 411-428.

Mansour, F., Wei, W., Danielson, N., 2013. Separation of carnitine and acylcarnitines in biological samples: A review. Biomed. Chromatogr. 27, 1339–1353.

Martinoia, S., Rosso, N., Grattarola, M., Lorenzelli, L., Margesin, B., Zen, M., 2001. Development of ISFET array-based microsystems for bioelectrochemical measurements of cell populations. Biosens. Bioelectron. 16(9-12), 1043–1050.

Matsumoto, K., Yamada, Y., Takahashi, M., Todoroki, T., Mizoguchi, K., Misaki, H., Yukl, H., 1990. Fluorometric determination of carnitine in serum with immobilized carnitine dehydrogenase and diaphorase. Clin. Chem. 36, 2072–2076.

Matsuo, T., Esashi, M., 1981. Methods of isfet fabrication. Sensors and Actuators 1, 77–96.

Moret, J., Moreira, F., Almeida, S., Sales, M., 2014. New molecularly-imprinted polymer for carnitine and its application as ionophore in potentiometric selective membranes. Mater. Sci. Eng. C 43, 481–487.

MOSFETs, 2006. , in: Physics of Semiconductor Devices. pp. 293–373.

Murphy, J., Marquardt, K., Shug, A., 1985. Valproic acid associated abnormalities of carnitine metabolism. Lancet. 325(8432), 820-821.

Obon, J., Buendia, B., Canovas, M., Iborra, J., 1999. Enzymatic cycling assay for D-carnitine determination. Anal. Biochem. 274, 34–39.

Paterson, N., 1967. Relative constancy of 24-hour urine volume and 24-hour creatinine output. Clin. Chim. Acta 18, 57–58.

Plioplys, A., Plioplys, S., 1995. Serum levels of carnitine in chronic fatigue syndrome: clinical correlates. Neuropsychobiology 32, 132–138.

Poghossian, A., 1992. The super-Nernstian pH sensitivity of Ta_2O_5-gate ISFETs. Sensors Actuators B. Chem. 7, 367–370.

Pormsila, W., Krahenbuhl, S., Hauser, P.C., 2010. Determination of carnitine in food and food supplements by capillary electrophoresis with contactless conductivity detection. Electrophoresis 31, 2186–2191.

Prieto, J., Andrade, F., Aldamiz-Echevarria, L., Sanjurjo, P., 2006. Determination of free and total carnitine in plasma by an enzymatic reaction and spectrophotometric quantitation spectrophotometric determination of carnitine. Clin. Biochem. 39, 1022–1027.

Ramsay, R., Gandour, R., Van Der Leij, F., 2001. Molecular enzymology of carnitine transfer and transport. Biochim. Biophys. Acta - Protein Struct. Mol. Enzymol. 1546(1), 21-43.

Ramsay, R., Naismith, J., 2003. A snapshot of carnitine acetyltransferase. Trends Biochem. Sci. 28(7), 343-346.

Rebouche, C., 2004. Kinetics, pharmacokinetics, and regulation of L-carnitine and acetyl-L-carnitine metabolism, in: Annals of the New York Academy of Sciences, 30–41.

Rebouche, C., Paulson, D., 1986. Carnitine metabolism and function in humans. Annu. Rev. Nutr. 6, 41–66.

Rothberg, J., Hinz, W., Rearick, T., Schultz, J., Mileski, W., Davey, M., Leamon, J., Johnson, K., Milgrew, M., Edwards, M., Hoon, J., Simons, J., Marran, D., Myers, J., Davidson, J., Branting, A., Nobile, J., Puc, B., Light, D., Clark, T., Huber, M., Branciforte, J., Stoner, I., Cawley, S., Lyons, M., Fu, Y., Homer, N., Sedova, M., Miao, X., Reed, B., Sabina, J., Feierstein, E., Schorn, M., Alanjary, M., Dimalanta, E., Dressman, D., Kasinskas, R., Sokolsky, T., Fidanza, J., Namsaraev, E., McKernan, K., Williams, A., Roth, G., Bustillo, J., 2011. An integrated semiconductor device enabling non-optical genome sequencing. Nature 475, 348–352.

Sakurabayashi, T., Miyazaki, S., Yuasa, Y., Sakai, S., Suzuki, M., Takahashi, S., Hirasawa, Y., 2008. L-carnitine supplementation decreases the left ventricular mass in patients undergoing hemodialysis. Circ. J. 72, 926–931.

Schimmenti, L., Crombez, E., Schwahn, B., Heese, B., Wood, T., Schroer, R., Bentler, K., Cederbaum, S., Sarafoglou, K., McCann, M., Rinaldo, P., Matern, D., di San Filippo, C., Pasquali, M., Berry, S., Longo, N., 2007. Expanded newborn screening identifies maternal primary carnitine deficiency. Mol. Genet. Metab. 90, 441–445.

Schmidt-Sommerfeld, E., Penn, D., Kerner, J., Bieber, L., 1989. Analysis of acylcarnitines in normal human urine with the radioisotopic exchange-high performance liquid chromatography (HPLC) method. Clin. Chim. Acta 181, 231–238.

Schneider, M., Galup-Montoro, C., 2010. CMOS analog design using all-region MOSFET modeling. Cambridge University Press., 292-365.

Seline, K., Johein, H., 2007. The determination of l-carnitine in several food samples. Food Chem. 105, 793–804.

Sharma, S., Black, S., 2009. Carnitine homeostasis, mitochondrial function and cardiovascular disease. Drug Discov. Today Dis. Mech. 6(1-4), e31-e39.

Stefan-Van Staden, R., Mashile, T., Mathabathe, K., Van Staden, J., 2009. Determination of (S)-(+)-ibuprofen using enantioselective, potentiometric membrane electrodes based on macrocyclic antibiotics. Instrum. Sci. Technol. 37, 197–203.

Takahashi, M., Ueda, S., Misaki, H., Sugiyama, N., Matsumoto, K., Matsuo, N., Murao, S., 1994. Carnitine determination by an enzymatic cycling method with carnitine dehydrogenase. Clin. Chem. 40, 817–821.

Tran, D., Pham, T., Wolfrum, B., Offenhausser, A., Thierry, B., 2018. CMOS-compatible silicon nanowire field-effect transistor biosensor: technology development toward commercialization. Mater. (Basel, Switzerland) 11(5), 26.

Van Hal, R.., Eijkel, J., Bergveld, P., 1996. A general model to describe the electrostatic potential at electrolyte oxide interfaces. Adv. Colloid Interface Sci. 69, 31–62.

Vaz, F., Wanders, R., 2002. Carnitine biosynthesis in mammals. Biochem. J. 361, 417–429.

Wan, L., Hubbard, R., 1998. Determination of free and total carnitine with a random-access chemistry analyzer. Clin. Chem. 44, 810–816.

Zammit, V., Ramsay, R., Bonomini, M., Arduini, A., 2009. Carnitine, mitochondrial function and therapy. Adv. Drug Deliv. Rev. 61(14), 1353-1362.

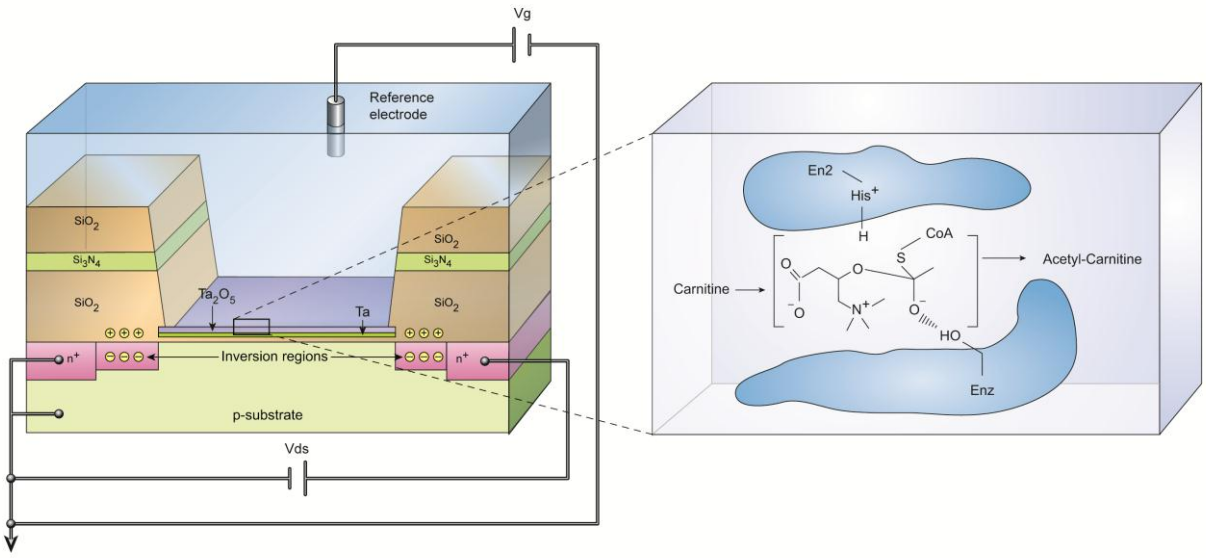

a

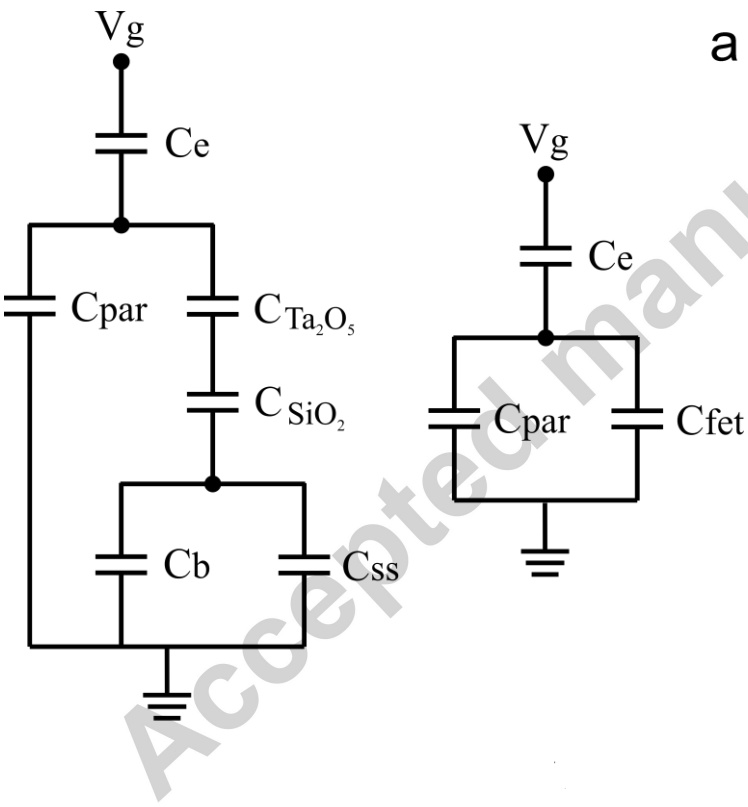

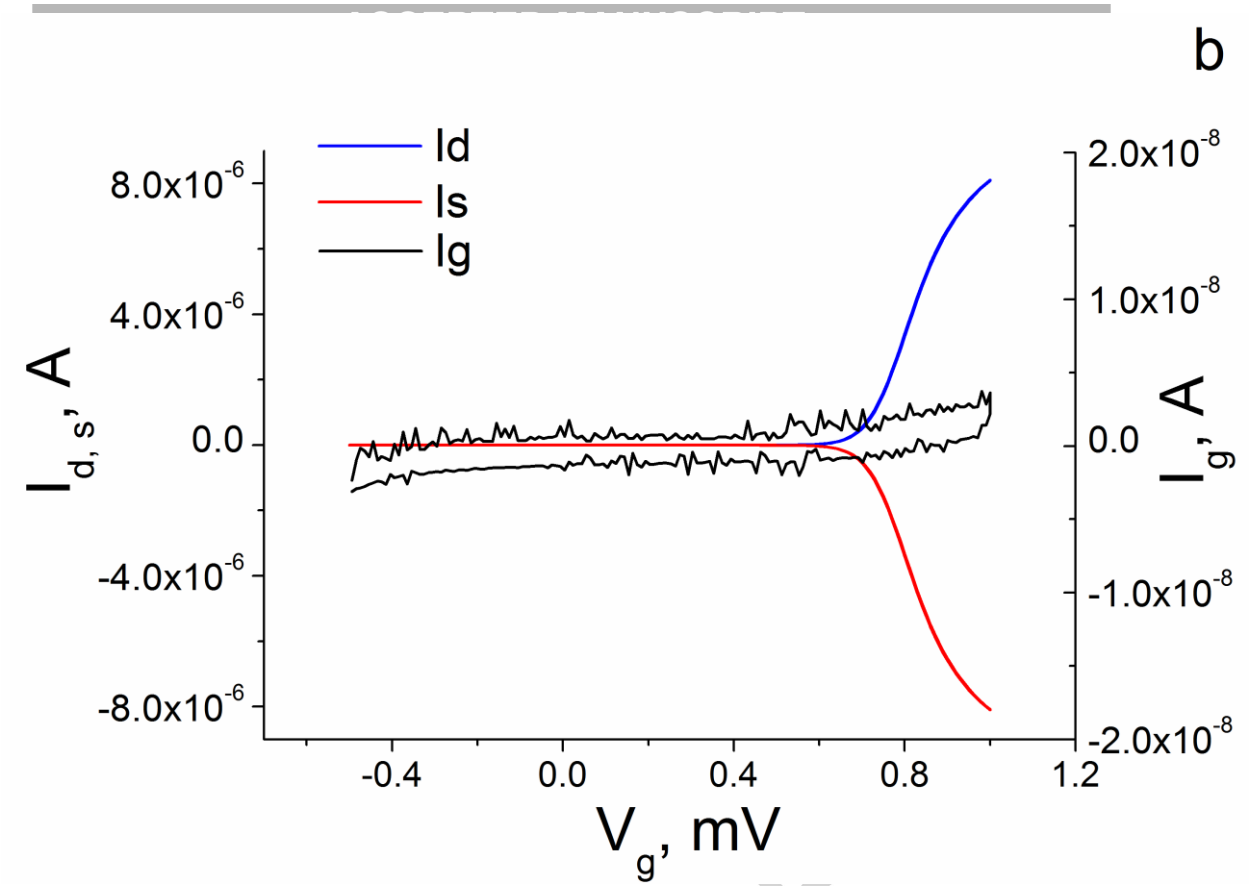
b
Id
Is
Ig
8.0x10-6
4.0x10-6
0.0
-4.0x10-6
-8.0x10-6
2.0x10-8
1.0x10-8
0.0
-1.0x10-8
-2.0x10-8
-0.4
0.0
0.4
0.8
1.2
Id, s, A
Ig, A
Vg, mV

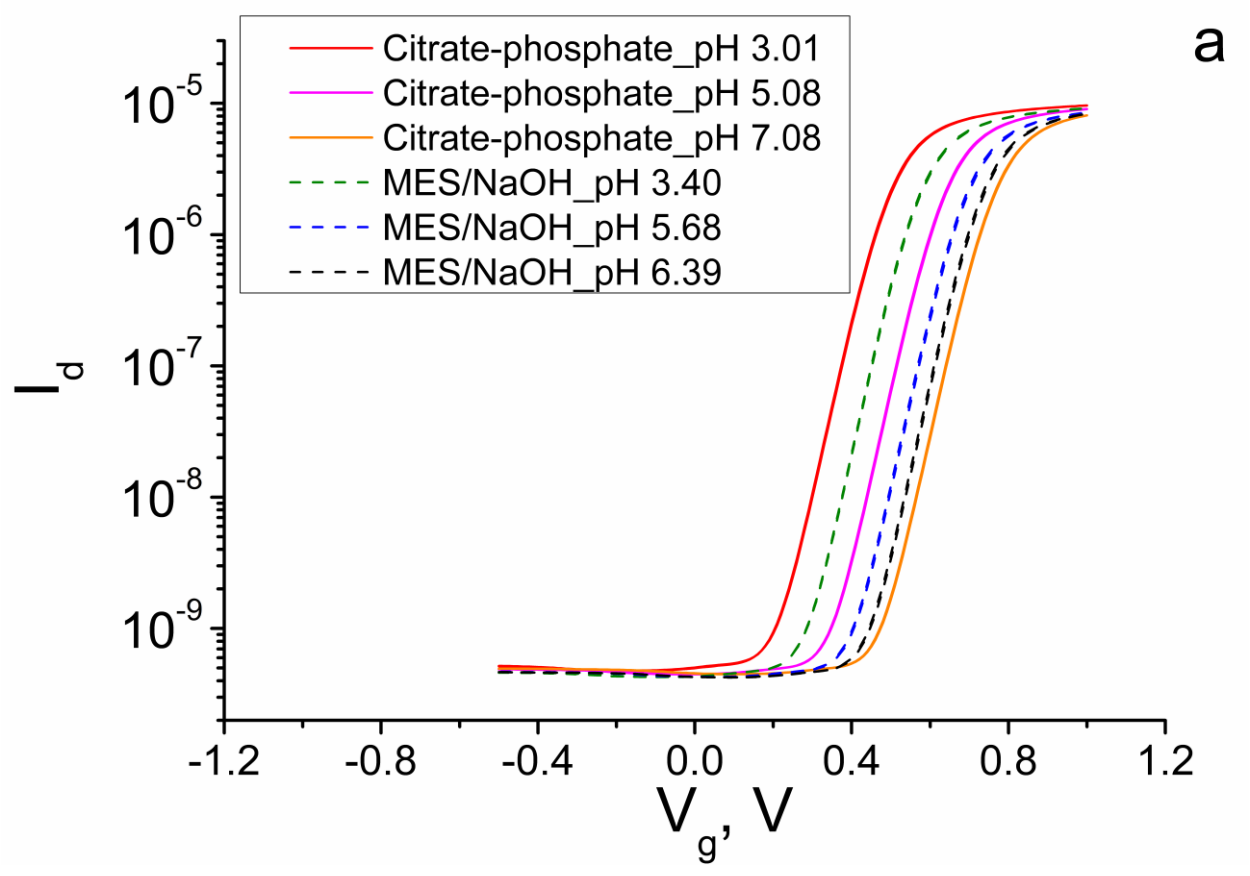
a
Citrate-phosphate_pH 3.01
Citrate-phosphate_pH 5.08
Citrate-phosphate_pH 7.08
MES/NaOH_pH 3.40
MES/NaOH_pH 5.68
MES/NaOH_pH 6.39
10-5
10-6
10-7
10-8
10-9
-1.2
-0.8
-0.4
0.0
0.4
0.8
1.2
Id
Vg, V

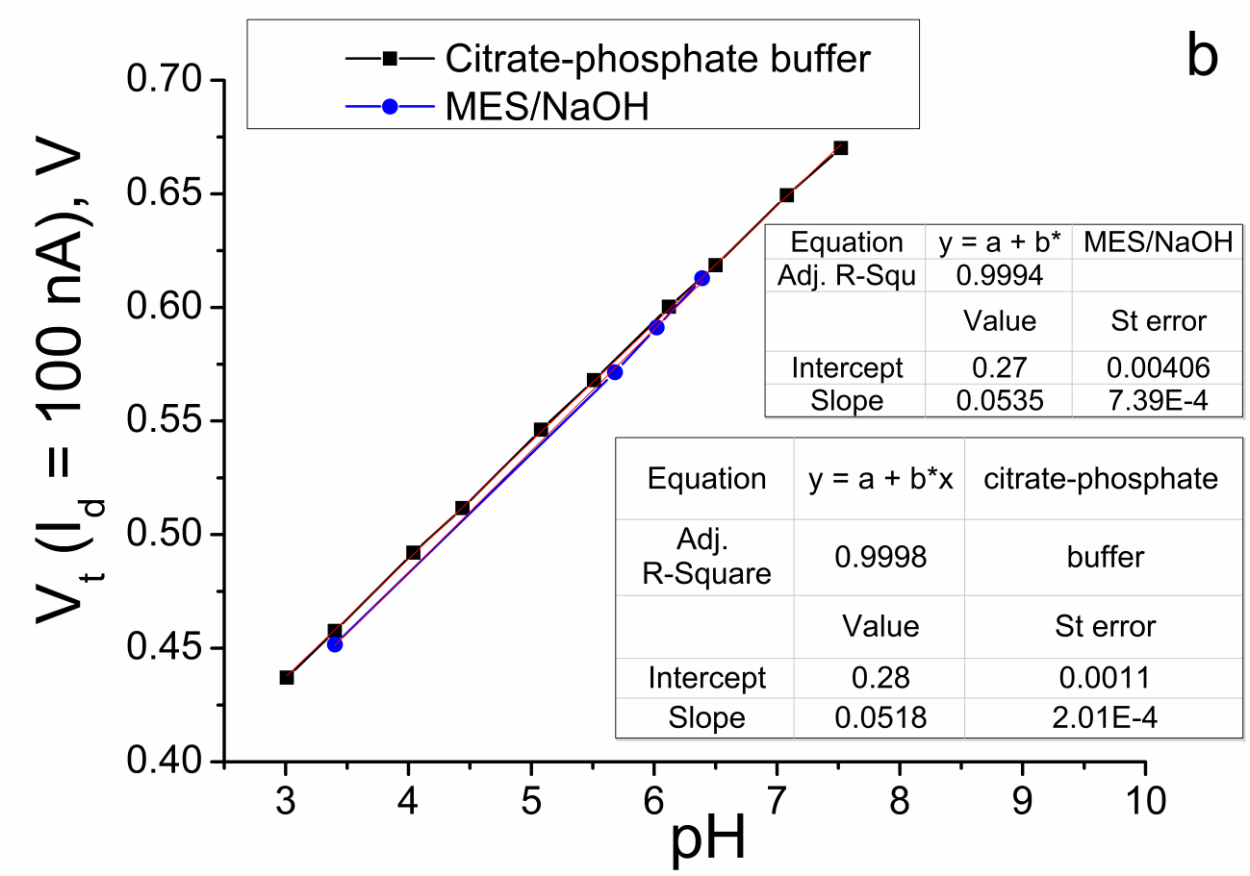

Equation	y = a + b*	MES/NaOH
Adj. R-Squ	0.9994	
	Value	St error
Intercept	0.27	0.00406
Slope	0.0535	7.39E-4

Equation	y = a + b*x	citrate-phosphate
Adj. R-Square	0.9998	buffer
	Value	St error
Intercept	0.28	0.0011
Slope	0.0518	2.01E-4

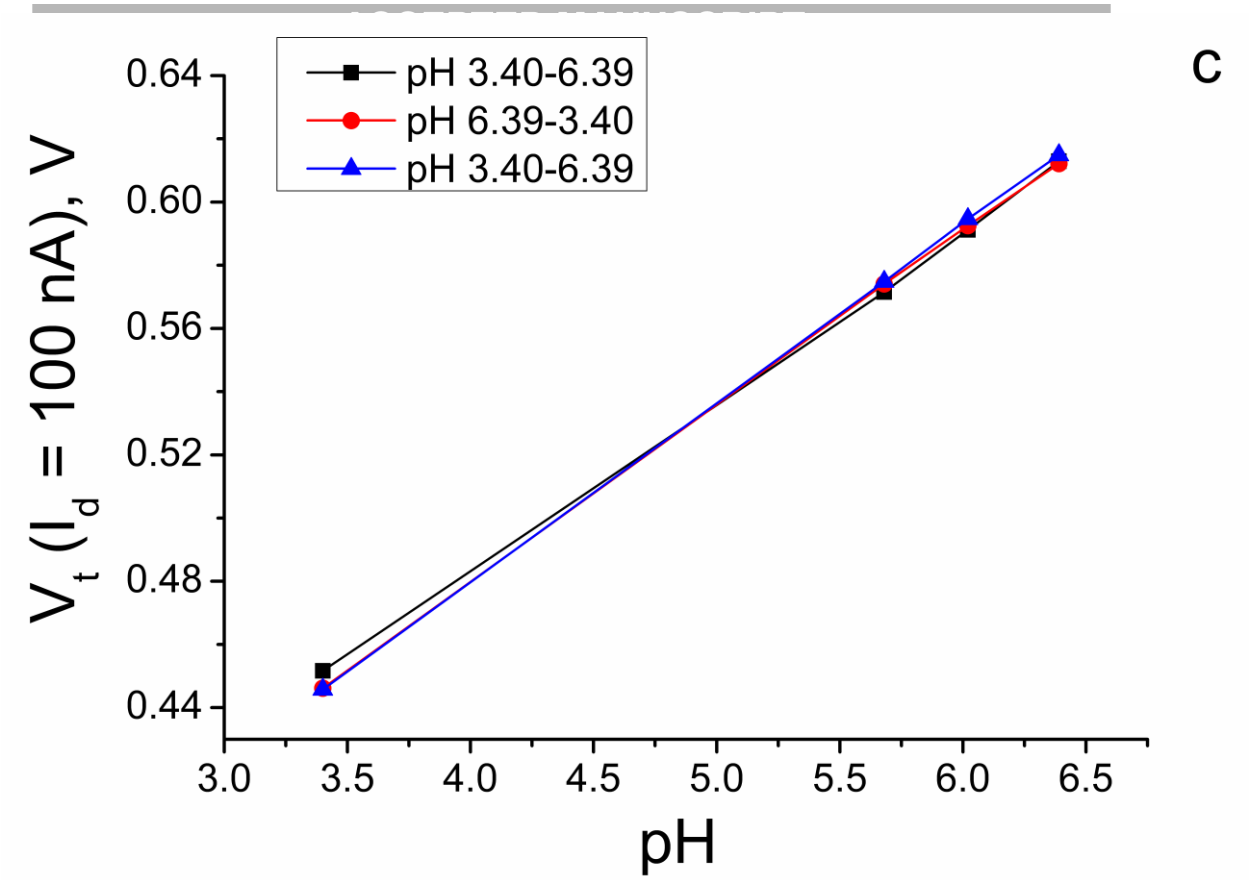
C
pH 3.40-6.39
pH 6.39-3.40
pH 3.40-6.39
V_t (I_d = 100 nA), V
0.64
0.60
0.56
0.52
0.48
0.44
3.0
3.5
4.0
4.5
5.0
5.5
6.0
6.5
pH

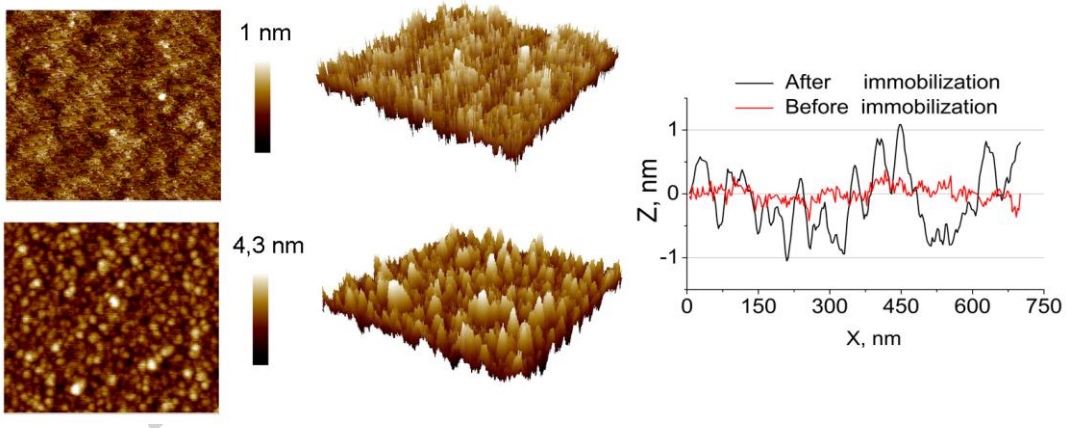
1 nm
4,3 nm
After immobilization
Before immobilization
Z, nm
1
0
-1
0
150
300
450
600
750
X, nm

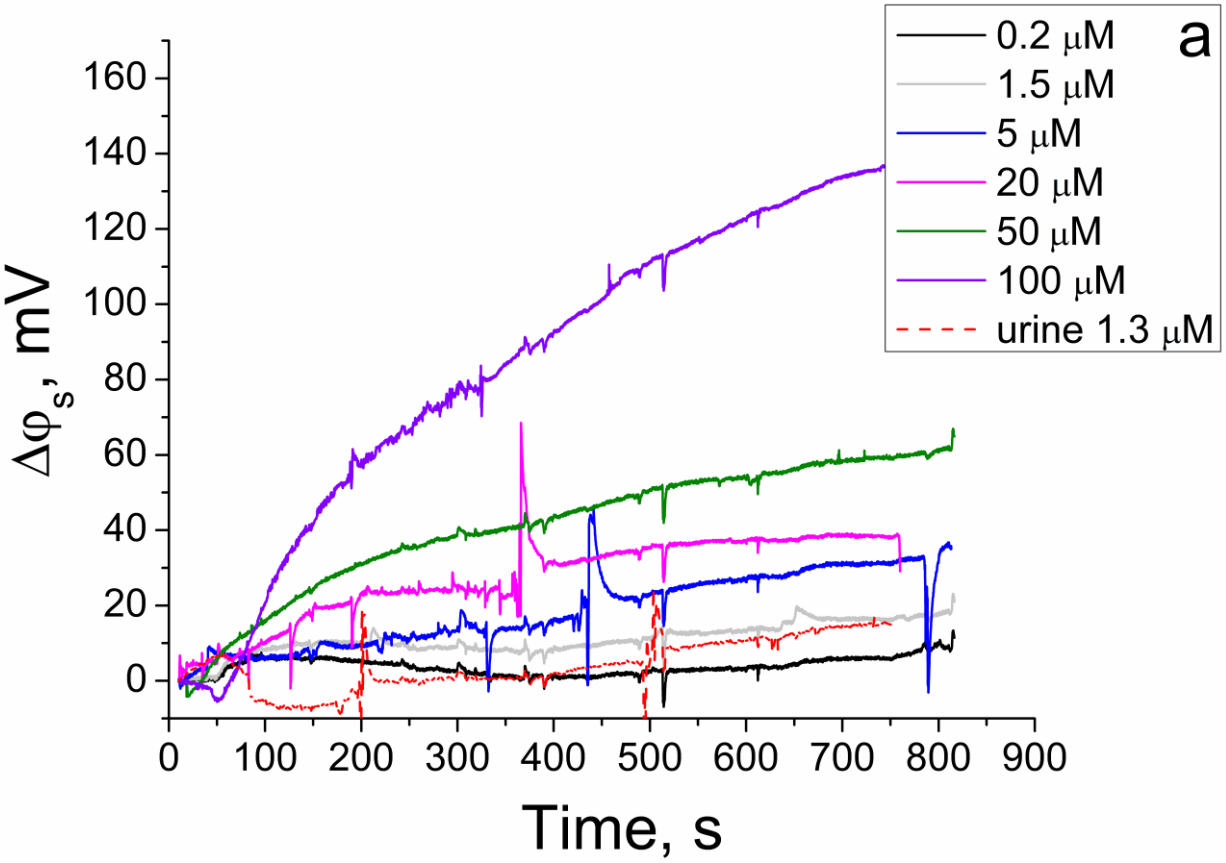
a
0.2 μM
1.5 μM
5 μM
20 μM
50 μM
100 μM
urine 1.3 μM
Δφs', mV
Time, s
0
20
40
60
80
100
120
140
160
0
100
200
300
400
500
600
700
800
900

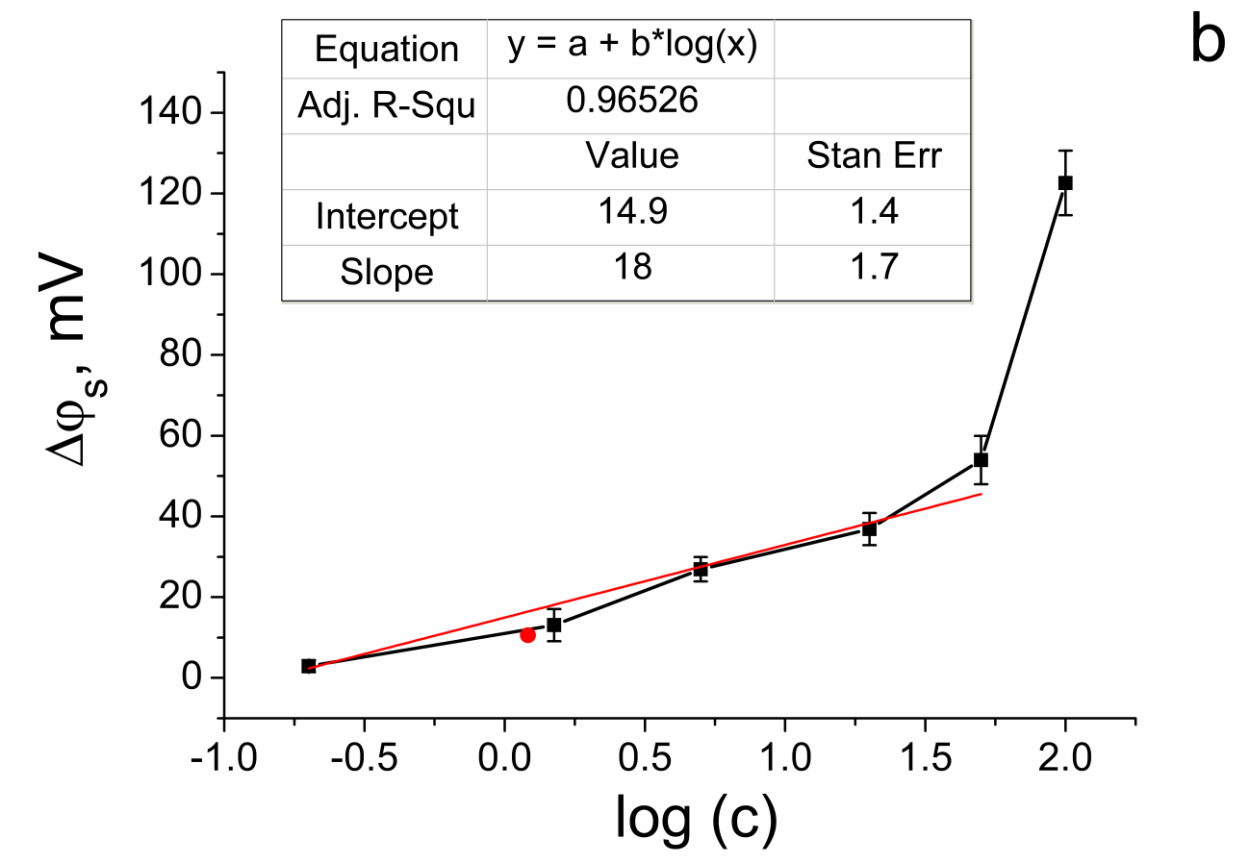
b
Equation
y = a + b*log(x)
Adj. R-Squ
0.96526
Value
Stan Err
Intercept
14.9
1.4
Slope
18
1.7
Δφs', mV
log (c)
0
20
40
60
80
100
120
140
-1.0
-0.5
0.0
0.5
1.0
1.5
2.0

Highlights

- A novel CMOS-compatible ISFET was developed and specially optimized for use in subthreshold operation mode.
- Carnitine acetyltransferase reaction was directly detected using an electrochemical method for the first time.
- The fabricated biosensor allowed detection of L-carnitine in artificial urine.